Journal of Molecular Liquids 416 (2024) 126465

Contents lists available at ScienceDirect

Journal of Molecular Liquids

journal homepage: www.elsevier.com/locate/molliq

Reinvestigation of the mechanism of the enamine-mediated dioxygen activation

Mihály Purgel [a], A. Jalila Simaan [b], Yongxing Wang [b], Marius Réglier [b], Michel Giorgi [c], József Kaizer [d,*]

[a] University of Debrecen, Egyetem tér 1, H-4032 Debrecen, Hungary
[b] Aix Marseille Université, Centrale Méditerranée, CNRS, iSm2 UMR 7313, 13397 Marseille, France
[c] Aix Marseille Université, CNRS, Centrale Méditerranée, FSCM UAR1739, 13397 Marseille, France
[d] Research Group of Bioorganic and Biocoordination Chemistry, University of Pannonia, 8201 Veszprém, Hungary

ARTICLE INFO

Keywords:
Enamine
Dioxygen activation
Hydroperoxides
Single electron transfer
Computation
Kinetics

ABSTRACT

The reaction of cyclohexylidene-2-carbamylcyclohex-1-enylamines with molecular oxygen does not undergo a [4+2] cycloaddition reactions but leads mainly to a dimer via single electron transfer (SET) from the enamine to $^3O_2$, proton transfer (PT) and consecutive radical C–C coupling, an addition to the formation of hydroperoxide byproduct.

1. Introduction

The electrocyclic [4+2] addition reaction of conjugated dienes with $^1O_2$ is a well-studied reaction and attracted great interest recently [1]. However, the similar reaction with triplet dioxygen is spin-forbidden [2], since organic compounds, and so conjugated dienes, are in the singlet state. According to that in normal cases conjugated dienes should not react with molecular oxygen [2]. It has been reported however, that some 2-aza-1,3-dienes (**1**) react with triplet dioxygen and the formation of the endoperoxides **2** have been claimed [3,4]. It has been found later, based on NMR studies, that **1** undergoes cyclisation and in the solution it has the cyclic form of **3** [5,6]. It has also been shown that the reaction of **3a** (R = H) with $^3O_2$ does not lead to **2a** but to a hydroperoxide [7,8] of the structure **6a** (R = Me) as showed by X-ray crystallography (Scheme 1) [9].

2. Experimental section

2.1. Materials and methods

Starting materials (cyclohexylidene-2-carbamylcyclohex-1-enylamines) are commercially available and they were purchased from Sigma-Aldrich. Cyclic voltammograms (CV) were taken on a VoltaLab 10 potentiostat with VoltaMaster 4 software for data process. The electrodes were as follows: glassy carbon (working), Pt (auxiliary), and Ad/AgCl with 3 M KCl. The potentials were referenced *vs.* the ferrocene/ferrocenium (Fc/Fc^+) redox couple. CV data were measured in argon saturated DMF using 0.1 M TBAP as electrolyte. IR spectra were recorded using a Thermo Nicolet Avatar 330 FT-IR instrument (Thermo Nicolet Corporation, Madison, WI, USA). Samples were prepared in the form of KBr pellets. ESR spectra were recorded on a Bruker ElexSys E500 X-band spectrometer. ESR conditions were as follows: microwave frequency: 9.8809 GHz; microwave power: 2 mW; modulation frequency: 100 kHz; modulation amplitude: 1 G; sweep width: 130 G centered at 3521 G; each spectrum was average of 20 scans. NMR spectrum was recorded on a Bruker Avance 400 spectrometer (Bruker Biospin AG, Fällanden, Switzerland). Microanalyses (elemental analysis) were done by the Microanalytical Service of the University of Pannonia. The crystals were mounted on a Nonius KappaCCD diffractometer. The structures were solved by SIR92 [10] and refined with the SHELXL [11] refinement package using Least Squares minimization. The hydrogen atoms were added at idealized positions and refined as riding atoms with their Uiso parameters constrained to 1.5Ueq (parent atoms) for the OH and the CH_3 groups and to 1.2Ueq (parent atoms) for the CH_2 and NH groups. In compound **6b**, the organic moiety co-crystallized with a methanol solvate.

* Corresponding author.
E-mail address: kaizer.jozsef@mk.uni-pannon.hu (J. Kaizer).

https://doi.org/10.1016/j.molliq.2024.126465
Received 19 July 2024; Received in revised form 5 November 2024; Accepted 6 November 2024
Available online 10 November 2024

2.2. Crystal data for compound **6b**

$C_{16}H_{29}Cl_1N_2O_4$, M_w = 348.86, monoclinic, space group $P2_1/n$, a = 11.5459(9), b = 10.1885(9), c = 15.779(1) Å, β = 89.559(5)°, V = 1856.1(2) Å^3, Z = 4, Dc = 1.25 g cm^{-3}, μ(Mo-Kα) = 0.226 cm^{-1}, 3744 reflections measured at 298 K, 213 parameters refined on F using 3744 unique reflections to final indices $R[F > 4\sigma(F)] = 0.0717$, $wR[F > 4\sigma(F)] = 0.1301$. The final residual Fourier positive and negative peaks were equal to 0.509 and −0.257, respectively. CCDC deposition code 222432.

2.3. Kinetic data for the reaction of enamines with dioxygen

Kinetic experiments were performed in $CHCl_3$ solutions at 25–40 °C at constant dioxygen pressure under pseudo-first-order conditions. The oxidation reactions, followed by volumetric measurements of the dioxygen uptake, afforded a time profile indicating that the reaction order with respect to the substrate **3** is one (Table S1). On the basis of the calculated V_H/V_D value of 1.02 (solvent isotope effect, SIE), determined kinetically (in the presence of 5 v/v% H_2O/D_2O). Peroxide content: 35 % for **3a** (R = H) and 30 % for **3b** (R = Me) based on iodometric titration.

2.4. Characterization

9a (R = H): Yield: (55–60 %). M.p.: 194 °C. FT-IR bands (KBr pellet, cm^{-1}) 3199, 3075, 2939, 2864, 2756, 1694, 1669, 1455, 1428, 1351, 1279, 1184, 1121, 1069, 1000, 956, 906, 831, 816, 779, 692, 676, 594, 522. $C_{26}H_{38}N_4O_2$: calcd. C 71.23; H 8.68; N 12.79; found: C 70.89; H 9.03; N 12.14.

9a.nHCl: ^{1}H NMR (400 MHz, D_2O-DCl-CD_3OD) δ (ppm): 4.81 (s, NH, 2H); 4.08–2.73 (m, 36H). ^{13}C NMR (100 MHz, D_2O-DCl-CD_3OD) δ (ppm): 20.16; 20.73; 21.07; 21.19; 21.65; 23.96; 24.32; 28.74; 32.55; 32.80; 33.01; 34.55; 36.97; 38.30; 38.82; 76.15; 78.77; 85.81; 95.02; 164.95 (C=N); 190.61 (C=O).

6b (R = Me): Yield: (30–35 %). M.p.: 199 °C. FT-IR bands (KBr pellet, cm^{-1}) 3195, 3073, 2939, 2864, 2753, 1690, 1667, 1455, 1425, 1345, 1275, 1231, 1179, 1121, 1069, 1000, 955, 906, 831, 812, 794, 690, 679, 592, 522. $C_{15}H_{24}N_2O_3$: calcd. C 64.26; H 8.63; N 9.99; found: C 64.14; H 8.79; N 10.04. GC–MS resulted the decay of the **6b** product into alcoholic form (264.10 (M^+, 6.15).

6b.nHCl: ^{1}H NMR (400 MHz, D_2O-DCl-CD_3OD) δ (ppm): 4.81 (s, NH, 2H); 4.06–2.63 (m, 34H); 2.48 (s, 2Me, 6H).

^{13}C NMR (100 MHz, D_2O-DCl-CD_3OD) δ (ppm): 20.12; 21.42; 26.76;

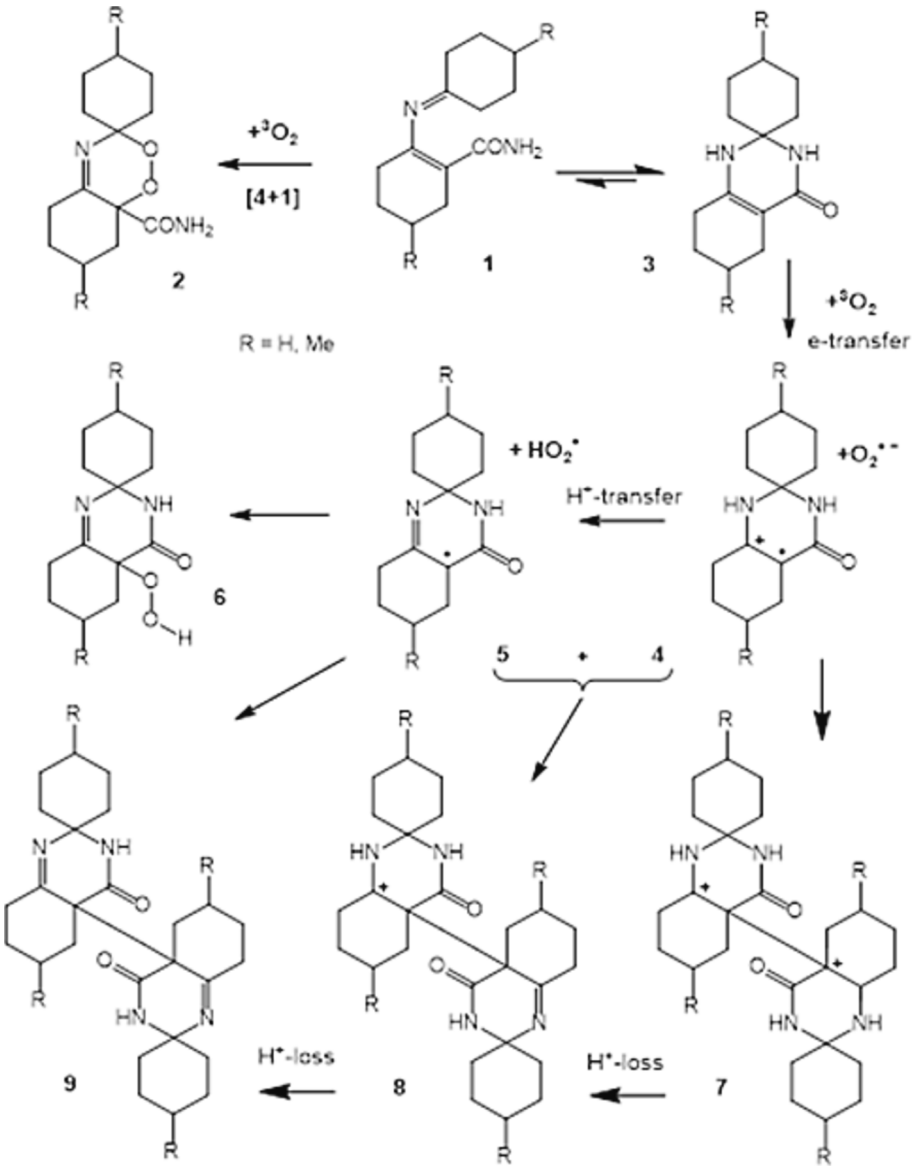

Scheme 1. The proposed reaction mechanism of the dioxygen activation of enamines. The main route is assigned by the thick arrows.

27.15; 28.72; 29.28; 31.06; 32.10; 35.71; 37.96; 38.62; 43.52; 75.36; 75.71; 78.32; 164.63 (C=N); 189.70 (C=O).

2.5. Computational methods

Plane Wave Density Functional Theory calculations were carried out by Quantum Espresso v.7.0 software package [12–14]. PBE (Perdew–Burke-Ernzerhof) functional [15] and Ultrasoft RRKJ (Rabe-Rappe-Kaxiras-Joanoupoulos algorithm) pseudopotential (PP) pseudopotential (_psl.0.1) were used for the geometry optimizations which were performed *in vacuo* http://pseudopotentials.quantum-espresso.org/legacy_tables. The Bravais-lattice index was 1 (simple or primitive cubic cell) where the k_x, k_y, and k_z points of the Brillouin zone were 1 1 1, and the cell size was 40 Bohr (21.17 Å). The kinetic energy cutoff for wavefunctions (ecutwfc) was 30.0 Rydberg, and the kinetic energy cutoff for charge density and potential for norm-conserving pseudopotential (ecutrho) was 300 Rydberg. To represent the structures of the molecules and clusters the Molekel program was used. DFT calculations were also performed by Gaussian software [16].

3. Results and discussion

We reinvestigated the reactions of **3a,b** (R = H and Me, respectively) with $^3O_2$ and found that the products (**9a,b**) were obtained, which were in all solvents very insoluble and from **3b** in a very small amount of the hydroperoxide **6b** could be occasionally isolated as the HCl adduct (Fig. 1) [17]. The compound has similar structural features as reported earlier for **6** [9].

The reaction of **3a** with triplet dioxygen gave a new compound **9a** in good yield (55–60 %), which turned out to be the dimer of **3a** (Fig. S1) [17]. The long C14–C16 (or C13–C13) bond distance of about 1.6 Å connecting the two monomers corresponds to a single bond between sp^3 hybridized carbon atoms. Based on this, we undertook DFT calculations for **9a** and showed that the optimized structures are consistent with the crystal structure (164 pm, Fig. 2).

The somewhat longer C–C bond length than that of the average lengths of such bonds is probably due to the steric strain in the dimer molecule. The formation of **9a,b** could be interpreted as a single electron transfer (SET) reaction from the enamines (**3a,b**) to dioxygen resulting in the radical cations **4a,b** and superoxide anion. Consecutive proton transfer from **4a,b** to superoxide anion gives the radical **5a,b**, which in a radical–radical coupling reaction ends up as the dimers **9a,b**. Radicals **5a,b** formed in the H^+-transfer reaction or in the slight dissociation of the dimers **9a,b** may also react with $HO_2^\bullet$ to the hydroperoxide **6a,b**. This reaction is however very limited and the hydroperoxide (**6a**) could only be isolated in small yields and only occasionally. Similar dimer formation was observed of the resonance-stabilized radicals from the antioxidant Irganox®HP-136 (5,7-di-*tert*-butyl-3-(3,4-dimethylphenyl)-3*H*-benzofuran-2-one) and 3,5-di-*tert*-butyl-4-hydroxyanisole after H-abstraction [18].

Since these isomers undergo C–C homolytic splitting only to a small extent, they are claimed to form a new type of antioxidants [19]. On the one hand, to our knowledge, H-abstraction from organic compounds by O_2 is not known in the literature. On the other hand, it is well-known that enamines are electron-rich olefins with a strong reduction potential. Despite the fact that the one electron reduction of $^3O_2$ is thermodynamically unfavorabde (E° = 1.265 V *vs.* Fc/Fc^+ in CH_2Cl_2, [20–22]) the strong reducing power of enamines (E° = −70–230 mV *vs.* Fc/Fc^+) proved by their redox potential [23–26], and photoelectron spectra [27]. The irreversible CVs of **1a** and **1b** with E° = 555 and 554 mV *vs.* Fc/Fc+ show obviously, that these enamines have sufficient potential to give up an electron to dioxygen forming an unstable cation [28,29] and superoxide anion (Fig. 3).

Literature data show that carbanions or radicals with electron affinities less than 20 kcal mol^{-1} react with ground state dioxygen [30]. Indeed, tests for the formation of superoxide anion by TNB (terazonium blue test [31]) were positive indicating the formation of $O_2^{\bullet-}$. Direct observation of radicals forming during the reaction was unsuccessful due to its short lifetime. Using DMPO (5,5-dimethyl-1-pyrroline-1-*N*-oxide) spin trap we observed a superimposed spectrum of two DMPO-radical adducts (Fig. 4) [32–34]. Species one is a carbon-centered radical adduct (g = 2.0051; a^N1 = 15.2 G; a^H1 = 18.3 G) formed probably from the radical **5a**. The other species is an oxygen-centred radical adduct (g = 2.0052; a^N1 = 14.0 G; a^H1 = 7.4 G; a^H2 = 1.8 G)

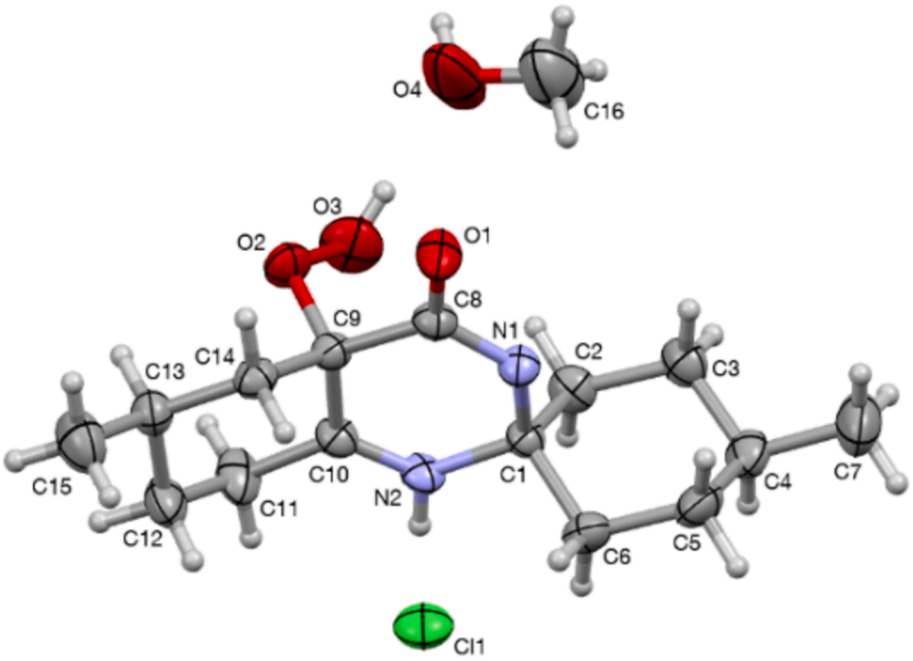

Fig. 1. The molecular structure of **6b** with selected bond distances (Å) and angles (°): O(1)-C(8) 1.233(3), O(2)-O(3) 1.456(3), O(2)-C(9) 1.430(3), N(1)-C(1) 1.453 (3), N(1)-C(8) 1.334(3), N(2)-C(1) 1.471(3), N(2)-C(10) 1.271(73), C(9)-C(10) 1.503(3), O(3)-O(2)-C(9) 106.71(19), N(1)-C(1)-N(2) 110.0(2), O(1)-C(8)-N(1) 122.0 (2), N(1)-C(8)-C(9) 118.9(2), C(8)-C(9)-C(10) 113.6(2).

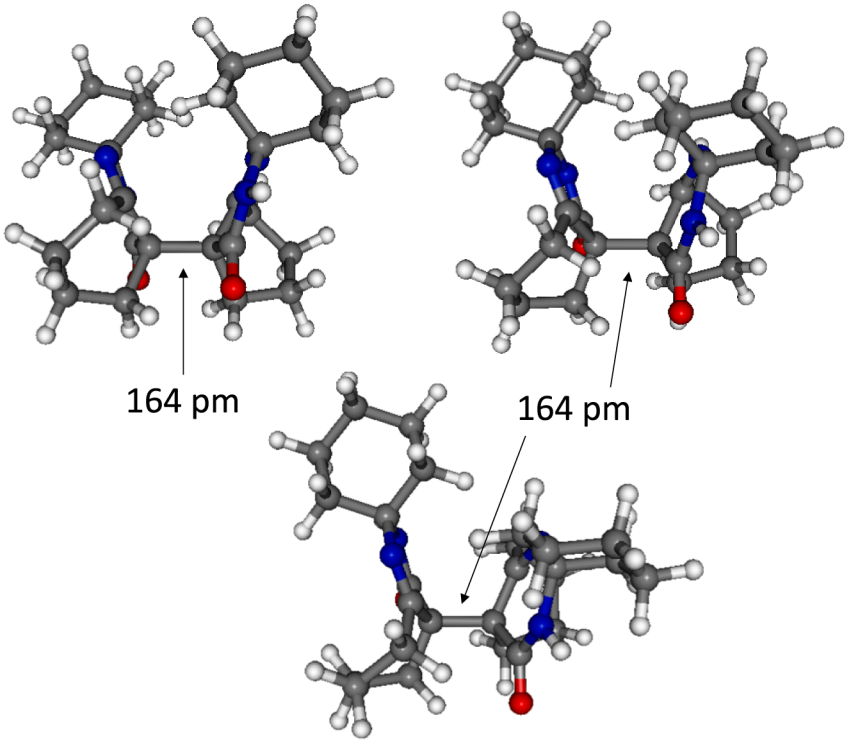

Fig. 2. The optimized molecular structure of **9a** in different orientations.

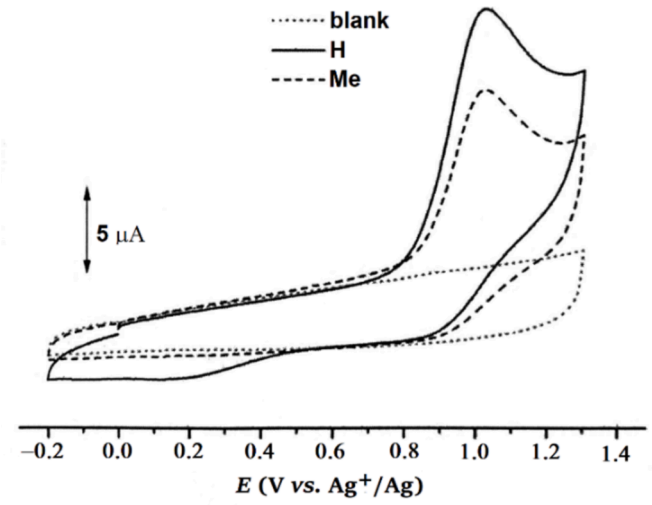

Fig. 3. The CVs of **3a** (R = H) and **3b** (R = Me).

very likely a result of superoxide radical trapping. The ratio of the two species is 3.3. The correlation coefficient of the fit is R = 0.995 [35].

Kinetic experiments were performed in $CHCl_3$ solutions at 25–40 °C at constant dioxygen pressure under pseudo-first-order conditions. The oxidation reactions, followed by volumetric measurements of the dioxygen uptake, afforded a time profile indicating that the reaction order with respect to the substrate **3b** is one (Fig. 5).

A straight line was obtained in a plot of the initial reaction rate *versus* the initial concentration of **3b** (Fig. 6A) and dioxygen (Fig. 6B) to establish a rate law of $-d[\mathbf{3b}]/dt = k[\mathbf{3b}][O_2]$ with kinetic parameters: k (**3b**) = (4.91 ± 0.25) × 10^{-2} M^{-1} s^{-1}, $\Delta H^{\ddagger} = 59$ kJ mol^{-1}, $\Delta S^{\ddagger} = -78$ J mol^{-1} K^{-1} at 308.16 K (Fig. S3) at 35 °C, and $\Delta G^{\ddagger} = 83$ kJ mol^{-1} was derived from it.

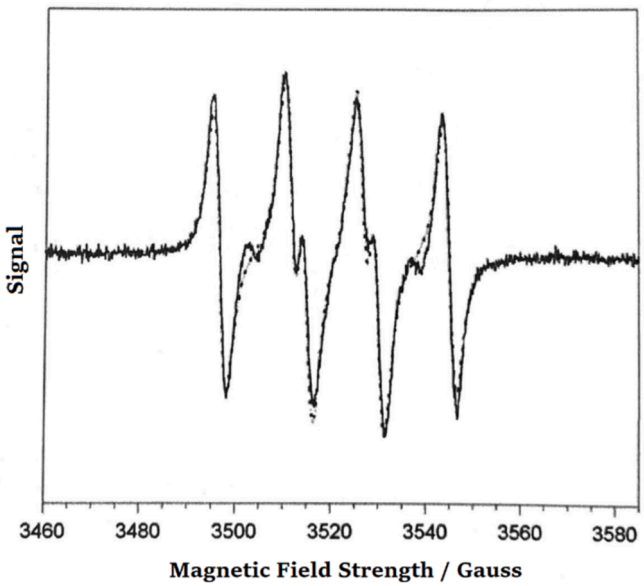

Fig. 4. The ESR spectra of the reaction mixture of **3a** with dioxygen in the presence of DMPO. Dotted line is the simulation.

Similar value has been found for **3a** (k (**3a**) = (4.31 ± 0.21) × 10^{-2} M^{-1} s^{-1}). The large negative entropy of activation indicates an associative mode of activation in the rate-determining step. On the basis of the calculated V_H/V_D value of 1.02 (solvent isotope effect, *SIE*), determined kinetically (in the presence of 5 v/v% H_2O/D_2O) the oxidation reaction is proposed to occur via an ET-PT (electron transfer-proton transfer) mechanism, where the ET is the rate-determining step [36–38]. The HAT (hidrogen atom transfer) can be clearly excluded.

DFT calculations were performed to study the reaction mechanism of the dimer formation and the products of the other pathways. By

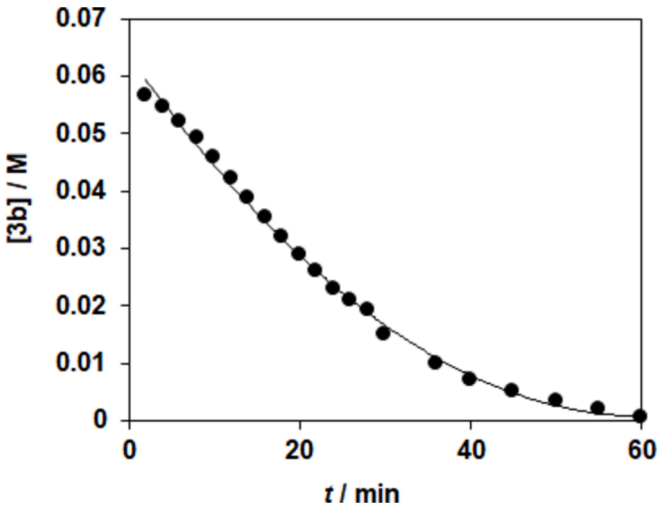

Fig. 5. Dioxygen activation by enamines. The time course in the oxidation of **3b** in $CHCl_3$ at 35 °C.

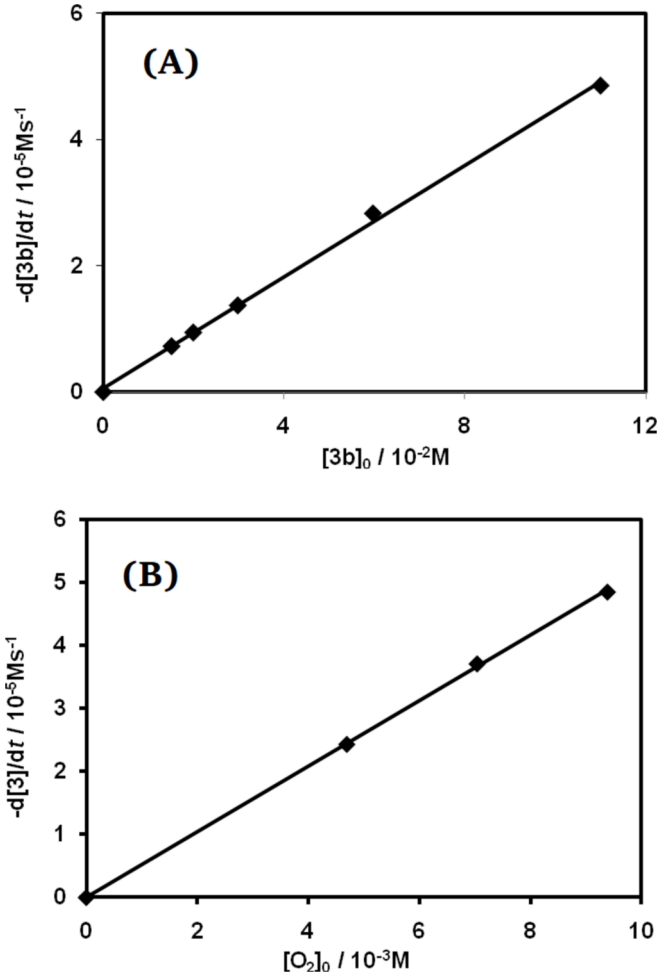

Fig. 6. Dioxygen activation by enamines in $CHCl_3$ at 35 °C. (A) Dependence of the initial rates on the concentration of **3b**. (B) Dependence of the initial rates on the dioxygen concentration.

comparing the total energies of the monomer products **2** and **6**, the formation of **6** was energetically unfavorable (+9.44 kJ mol^{-1}); however, experimentally it was found that the reaction of enamines with $^3O_2$ does not lead to cycloreaction. Furthermore, the formation of **3** was, less favorable than that of **2** but it is worth mentioning that the activation barrier of the addiction of $^3O_2$ to the enamine (**1** → **2**) seems to be kinetically inferior to the **1** → **3** cyclization reaction but the transition states of the elementary steps were not studied. The formation of **2**, **3,** and **6** are described in the Eqs. (1)–(6). Since the **1** → **3** equilibrium is strongly shifted towards the formation of **3**, an electron transfer from **3** to $^3O_2$ followed by a proton transfer to $^3O_2^{\bullet-}$ is noteworthy due to the non-existence of **2**. The separate molecule model resulted in very high energies for the formation of **4** and **5** due to the not well-defined parameters of spin in PW DFT calculations. To solve this problem, the small molecules ($^3O_2$, $^3O_2^{\bullet-}$, $HO_2^{\bullet}$) were added to the species **3**, **4** and **5** to form adducts, respectively. Since the formation **4** and **5** from **3** showed very high energy by comparing the energy of separated molecules (see Eqs. (7) and (8)), it was noteworthy to study clusters where there was weak interactions between the molecules. In this cluster model the ion pair [**4** + $^3O_2^{\bullet-}$] could not be found as a minimum since it converged to [**3** + $^3O_2$], however; [**5** + $HO_2^{\bullet}$] was observed, and its energy was +127.1 kJ mol^{-1} higher than that of [**3** + $^3O_2$], Eq. (9). Direct comparison of **4** + $^3O_2^{\bullet-}$ and **5** + $HO_2^{\bullet}$ was possible by the separate molecule model, and it was found that **5** + $HO_2^{\bullet}$ had +40.6 kJ mol^{-1} higher energy referred to **4** + $^3O_2^{\bullet-}$, Eq. (10). It means that the formation of free $HO_2^{\bullet}$ by deprotonating a monomer cationic radical species was unfavorable. The dimerization was studied in two cases: [4+**4**] and [**5** + **5**] clusters were compared to the dimer forms **7** and **9**, see Eqs. (11), (12). Gaussian calculation at different theoretical levels showed also unfavorable energies (ΔG_r ~300 kJ mol^{-1} *in vacuo*; ΔG_r = +144 kJ mol^{-1} at M062X/TZVP/SMD in chloroform) for (7) but resulted in significantly smaller value (~40 kJ mol^{-1} *in vacuo*; and +67 kJ mol^{-1} at M062X/TZVP/SMD in chloroform) for (8) by using the separate molecule model. We can assume that a reasonable value for the formation of **4** could be derived by combining the energies Eqs. (9) and (10) calculated by PW. It means that by eliminating the ΔG_r of (10) from (9) it results in +86.5 kJ mol^{-1} which is, however; only a fictive approximation but a derived $\Delta G^{\ddagger}_{calc}$ shows a good agreement with the derived experimental value ($\Delta G^{\ddagger}_{exp}$ = +83 kJ mol^{-1}). It depends, however; on the λ value used for the Marcus' theory (e.g. λ = 1.5 then $\Delta G^{\ddagger}_{calc}$ = 92kJ mol^{-1}) according to $\Delta G^{\ddagger} = \frac{(\Delta G^0+\lambda)^2}{4\lambda}$ Furthermore, the bond dissociation energy (BDE) of **9** (122.1 kJ mol^{-1}) which belongs to the long C–C bond, showed good agreement with the BDE energies found in the literature (95–110 kJ mol^{-1}) [39]. The BDE of **7** was also reasonable (57.4 kJ mol^{-1}) therefore it can be assumed that the formation of **7** and **8** charged dimers is also possible. Gaussian showed, however; only 42.3 kJ mol^{-1} for BDE of **9** by using separate model (**5** + **5** → **9**) while the cluster model (12) resulted in 65.9 kJ mol^{-1}. Note, that in the latter case, the monomers had different orientation to each other from the one optimized by Quantum Espresso. The deprotonation of **7** resulting in **9** was energetically favored, see Eq. (13). The C–C bond was 164, 166, and 166 pm in **7**, **8**, and **9**, respectively, while in the clusters, the C–C distance increased up to 417–433 pm. The proposed mechanism of the dimerization and the minor reaction pathways can be seen in Scheme 1 while the optimized structure of **9a** is in Fig. 2.

1 + $^3O_2$ → **2** ΔE = −89.0 kJ mol^{-1} (1)

[**1** + $^3O_2$] → **2** ΔE = −94.6 kJ mol^{-1} (2)

1 → **3** ΔE = −43.9 kJ mol^{-1} (3)

[**1** + $^3O_2$] → [**3** + $^3O_2$] ΔE = −40.4 kJ mol^{-1} (4)

1 + $^3O_2$ → **6** ΔE = −79.5 kJ mol^{-1} (5)

[**1** + $^3O_2$] → **6** ΔE = −85.2 kJ mol^{-1} (6)

3 + $^3O_2$ → **4** + $^3O_2^{\bullet-}$ ΔE = +512.5 kJ mol^{-1} (7)

3 + $^3O_2$ → **5** + $HO_2^{\bullet}$ ΔE = +553.1 kJ mol^{-1} (8)

$$[\mathbf{3} + {}^3O_2] \rightarrow [\mathbf{5} + HO_2^{\bullet}] \quad \Delta E = +127.1 \text{ kJ mol}^{-1} \tag{9}$$

$$\mathbf{4} + {}^3O_2^{\bullet-} \rightarrow \mathbf{5} + HO_2^{\bullet} \quad \Delta E = +40.6 \text{ kJ mol}^{-1} \tag{10}$$

$$[\mathbf{4} + \mathbf{4}] \rightarrow \mathbf{7} \quad \Delta E = -57.4 \text{ kJ mol}^{-1} \tag{11}$$

$$[\mathbf{5} + \mathbf{5}] \rightarrow \mathbf{9} \quad \Delta E = -122.1 \text{ kJ mol}^{-1} \tag{12}$$

$$\mathbf{7} + 2\ {}^3O_2^{\bullet-} \rightarrow \mathbf{9} + 2\ HO_2^{\bullet} \quad \Delta E = -25.8 \text{ kJ mol}^{-1} \tag{13}$$

4. Conclusion

We believe that the formation of both compounds, the hydroperoxide **6b** and the dimer **7a**, proceeds via similar intermediates and their mechanism can be interpreted as shown in Scheme 1. The ratio of oxygenation/dimerization is very small so that under the conditions applied the dimerization is the main reaction pathway. In summary, the results outlined above suggest clearly that the reaction of enamines with $^3O_2$ does not lead exclusively to the corresponding peroxides (**2a,b**). Single electron transfer to molecular oxygen takes place resulting in radical cations (**4a,b**) and superoxide anion. The consecutive proton transfer from **4a,b** to superoxide anion leads to neutral radicals (**5a,b**) and $HO_2^{\bullet}$. The formers may dimerize to the dimers (**9a,b**) or in reaction with $HO_2^{\bullet}$ end up in the hydroperoxides (**6a,b**).

5. Notes

To the memory of Professor Gábor Speier.

CRediT authorship contribution statement

Mihály Purgel: Formal analysis, Data curation. **A. Jalila Simaan:** Writing – review & editing, Supervision. **Yongxing Wang:** Investigation, Data curation. **Marius Réglier:** Writing – review & editing, Supervision. **Michel Giorgi:** Resources, Data curation. **József Kaizer:** Writing – review & editing, Writing – original draft, Supervision, Methodology, Conceptualization.

Declaration of competing interest

The authors declare that they have no known competing financial interests or personal relationships that could have appeared to influence the work reported in this paper.

Acknowledgements

Financial support of the Hungarian National Research, Development and Innovation Fund, OTKA K142212 (J.K.), TKP2021-NKTA-21 (J.K.) are gratefully acknowledged. Thanks to Dr. Péter Pál Fehér for the technical support. We acknowledge KIFÜ for awarding us access to resource based in Hungary.

Appendix A. Supplementary data

Supplementary data to this article can be found online at https://doi.org/10.1016/j.molliq.2024.126465.

Data availability

Data will be made available on request.

References

[1] A.G. Leach, K.N. Houk, Diels-Alder and ene reactions of singlet oxygen, nitroso compounds and triazolinediones: transition states and mechanisms from contemporary theory, Chem. Commun. 1243–1255 (2002).
[2] H. Taube, JPG, Mechanisms of Oxidation with Oxygen, 49 (1965) 29-50.
[3] A.F. McKay, E.J. Tarlton, C. Podesva, Novel condensation of cyclohexanone with urea, J. Org. Chem. 26 (1961) 76–79.
[4] A. F. Kay, J-M. Billy, E. J. Tarlton, Peroxides. Spiro[cyclohexane-1',3-9-carbamyl-3 (H)-5,6,7,8-tetrahydrobenzo-1, 2,4-dioxazines]. J. Org. Chem. 29 (1964) 291-294.
[5] G. Zigauner. G. Gubitz, β-Carbamoyl enamines: 5′. 6′. 7′. 8-Yetrahydrospiro [cyclohexane-1, 2′(1′ H)-quinazoline]-4′(3′ H)-one.(Heterocycles, XXIII) Über Heterocyclen, 23. Mitt. Mh. Chem. 101 (1970) 1547-1558.
[6] B. Witkop, J.B. Patrick, The course and kinetics of the acid-base-catalyzed rearrangements of 11-hydroxytetrahydrocarbazolenine, J. Am. Chem. Soc. 73 (1951) 2188–2195.
[7] Ch. Bischoff, Eine Ungewöhnliche Peroxidreaktion an einem Octahydrochinazolinon, J. Prakt. Chem. 318 (1976) 848–854.
[8] Ch. Bischoff, H. Herma, E. Schröder, Zur Synthese von Octahydrochinazolinonen und deren Reaktion mit Persäure, J. Prakt. Chem. 318 (1976) 895–901.
[9] K.J. McCullough, 5',6',7',8'-Tetrahydro-4a'-hydroperoxyspiro[cyclohexane-1,2'(2'H)-quinazoline]-4'(3'H)-one, Acta Cryst. C 42 (1986) 688–690.
[10] A. Altomare, G. Cascarano, C. Giacovazzo, A. Guagliardi, M.C. Burla, G. Polidori, M. Camalli, SIR92 - a program for automatic solution of crystal structures by direct methods, J. Appl. Crystallogr. 27 (1994) 435.
[11] G.M. Sheldrick, Crystal Structure Refinement with SHELXL, Acta Cryst. C 71 (2015) 3–8.
[12] P. Giannozzi, et al., QUANTUM ESPRESSO: a modular and open-source software project for quantum simulations of materials, J. Phys.: Condens. Matter 21 (2009) 395502.
[13] P. Giannozzi, et al., Advanced capabilities for materials modelling with Quantum ESPRESSO, J. Phys.: Condens. Matter 29 (2017) 465901.
[14] P. Giannozzi, et al., Quantum ESPRESSO toward the exascale, J. Chem. Phys. 152 (2020) 154105.
[15] a) J.P. Perdew, K. Burke, M. Ernzerhof, Generalized gradient approximation made simple, Phys. Rev. Lett. 77 (1996) 3865;
b) J.P. Perdew, K. Burke, M. Ernzerhof, Generalized gradient approximation made simple, Phys. Rev. Lett. 78 (1997) 1396.
[16] M.J. Frisch, et al., Gaussian 16, revision A.03, Gaussian Inc., Wallingford, CT, 2016.
[17] Deposition numbers CCDC 222432 (for **6b**) contains the supplementary crystallographic data for this paper. These data are provided free of charge by the joint Cambridge Crystallographic Data Centre and Fachinformationszentrum Karlsruhe Access Structures service. The crystal structure of **9a** was not published because of low quality data. However, its connectivity was clearly established. See supplementary material.
[18] M. Frenette, P.D. MacLean, L.R.C. Barclay, J.C. Scaiano, Radically different antioxidants: thermally generated carbon-centered radicals as chain-breaking antioxidants, J. Am. Chem. Soc. 128 (2006) 16432–16433.
[19] H.G. Korth, Carbon radicals of low reactivity against oxygen: radically different antioxidants, Angew. Chem. Int. Ed. 46 (2007) 5274–5276.
[20] D.T. Sawyer, Oxygen Chemistry, Oxford University Press, New York, 1991, p. 34.
[21] M.E. Peover, B.S. White, The formation of the superoxide ion by electrolysis of oxygen in aprotic solvents, J. Chem. Soc., Chem. Commun. (1965) 183–184.
[22] J. Ruiz, D. Astruc, Permethylated electron-reservoir sandwich complexes as references for the determination of redox potentials. Suggestion of a new redox scale, C.R. Acad. Sci. Ser. Iic: Chim. 1 (1998) 21–27.
[23] G. Cook, Enamines: Synthesis, Structure, and Reactions, 2nd ed., Marcel Dekker, New York, 1988, p. 248.
[24] J.M. Fritsch, H. Weingarten, J.D. Wilson, Electrolytic oxidations of organic compounds. II. N,N-dimethylaminoalkenes. J. Am. Chem. Soc. 92 (1970) 4038-4046.
[25] M. Schaemann, H.J. Schaefer, Reaction of enamines and mediated anodic oxidation of carbohydrates with the 2,2,6,6-tetramethylpiperidine-1-oxoammonium ion (TEMPO+), Electrochim. Acta 50 (2005) 4956–4972.
[26] F.R. Perez, L. Basáez, J. Belmar, P. Vanisek, J. Chil. Chem. Soc. 50 (2005) 575.
[27] B. Cetinkaya, G.H. King, S.S. Krishnamurty, M.F. Lappert, J.P. Pedley, Photoelectron spectra of electron-rich olefins and an isostructural boron compound; olefins of exceptionally low first ionisation potential, J. Chem. Soc., Chem. Commun. (1971) 1370–1471.
[28] K. Blau, V. Voerckel, Studies on the oxidation of enamines with molecular oxygen. I. Oxidation of some piperidino alkenes, J. Pract. Chem. 331 (1989) 285–292.
[29] R. Beel, S. Kobialka, M.L. Schmidt, M. Engeser, Direct experimental evidence for an enamine radical cation in SOMO catalysis, Chem. Commun. 47 (2011) 3293–3295.
[30] C.H. DePuy, V.M. Bierbaum, L.A. Flippin, J.J. Grabowski, G.K. King, R.J. Schmitt, Generation of specific isomeric carbanions in the gas phase, J. Am. Chem. Soc. 101 (1979) 6443.
[31] H. Vezin, E. Lamour, S. Routier, F. Villain, C. Bailly, J.-L. Bernier, J.P. Catteau, Free radical production by hydroxy-salen manganese complexes studied by ESR and XANES, J. Inorg. Biochem. 92 (2002) 177–182.
[32] M. Mojovic, I. Spasojevic, M. Vuletic, Z. Vucinic, G. Bacic, An EPR spin-probe and spin-trap study of the free radicals produced by plant plasma membranes, J. Serb. Chem. Soc. 70 (2005) 177–186.
[33] G.R. Buettner, On the reaction of superoxide with DMPO/OOH, Free Rad. Res. Commun. 10 (1990) 11–15.
[34] S.S. Eaton, G.R. Eaton, L.J. Berliner, Biomed. EPR 23 (2005) 80.
[35] F. Neese, The ORCA program system, WIRES Comput. Mol. Sci. 2 (2012) 73.
[36] Z. Markovic, J. Dorovic, M. Dekic, M. Radulovic, S. Markovic, M. Ilic, DFT study of free radical scavenging activity of erodiol, Chem. Papers 67 (2013) 1453–1461.

[37] M. Bietti, M. Salamone, Kinetic solvent effects on hydrogen abstraction reactions from carbon by the cumyloxyl radical. The role of hydrogen bonding, Org. Lett. 12 (2010) 3654–3657.
[38] J.M. Mayer, I.J. Rhile, Thermodynamics and kinetics of proton-coupled electron transfer: stepwise vs. concerted pathways, Biochim. Biophys. Acta 1655 (2004) 51–58.
[39] M. Frenette, C. Aliaga, E. Font-Sanchis, J.C. Scaiano, Bond dissociation energies for radical dimers derived from highly stabilized carbon-centered radicals, Org. Lett. 6 (2004) 2579–2582.